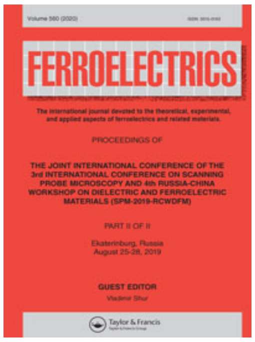

Ferroelectrics

ISSN: 0015-0193 (Print) 1563-5112 (Online) Journal homepage: https://www.tandfonline.com/loi/gfer20

Temperature dependence of the spontaneous polarization, acoustic and strain anomalies in strontium barium niobate crystals of different chemical compositions probed by the second harmonic generation technique

A. M. Pugachev, I. V. Zaytseva, V. K. Malinovsky, N. V. Surovtsev, M. V. Gorev, L. I. Ivleva & P. A. Lykov

FERROELECTRICS
2020, VOL. 560, 54–60
https://doi.org/10.1080/00150193.2020.1722883

Temperature dependence of the spontaneous polarization, acoustic and strain anomalies in strontium barium niobate crystals of different chemical compositions probed by the second harmonic generation technique

A. M. Pugachev[a], I. V. Zaytseva[a], V. K. Malinovsky[a], N. V. Surovtsev[a], M. V. Gorev[b,c], L. I. Ivleva[d], and P. A. Lykov[d]

[a]Institute of Automation and Electrometry, Russian Academy of Sciences, Novosibirsk, Russia; [b]Kirensky Institute of Physics Federal Research Center KSC SB RAS, Krasnoyarsk, Russia; [c]Institute of Engineering Physics and Radioelectronics, Siberian Federal University, Krasnoyarsk, Russia; [d]Prokhorov General Physics Institute, Russian Academy of Sciences, Moscow, Russia

ABSTRACT
In $Sr_xBa_{1-x}Nb_2O_6$ crystals ($x = 0.33$, 0.5, 0.61, and 0.75), temperature dependences of spontaneous polarization, strain, elastic modules, and second harmonic generation (SHG) signal are compared. It is revealed that SHG describes the temperature dependences of dipole moments in polar nanoregions in paraelectric phase. In the vicinity of the phase transition in paraelectric phase, SHG reflects the temperature behavior of relatively large and long-lived polar asymmetric regions as indicated by the presence of the intermediate temperature range on the temperature dependence of this nonlinear response.

ARTICLE HISTORY
Received 28 August 2019
Accepted 25 November 2019

KEYWORDS
SBN-x crystals; polar regions; ferroelectric phase transition; second harmonic generation; Brillouin spectroscopy

1. Introduction

A number of studies have shown that nonlinear-optical investigations, in particular, the generation of the second optical harmonic, can effectively describe the behavior of dipole moments in ferroelectric crystals [1–3]. In most perovskites, the signal of the optical second harmonic generation (SHG) $I^{(2\omega)}$ is proportional to the square of spontaneous polarization P_s^2 in the ferroelectric phase [1,2].

It was natural to assume that SHG signals in the paraelectric centrosymmetric phase of ferroelectric crystals and relaxors ($PbMg_{1/3}Nb_{2/3}O_3$, $BaTiO_3$, $Sr_xBa_{1-x}Nb_2O_6$ (SBN-x) were also proportional to the square of values of local dipole moments P_d (in so-called polar nanoregions or PNR [4–6]). Non-centrosymmetric polar nanoregions are responsible for many unusual properties of ferroelectric crystals, which include not only relaxors, for example, $PbMg_{1/3}Nb_{2/3}O_3$ (PMN), but also ferroelectrics with some relaxor properties in particular, $Sr_xBa_{1-x}Nb_2O_6$ (SBN-x) and $BaTiO_3$ [4–10]. These non-centrosymmetric polar nanoregions are responsible for many unusual properties of these ferroelectric crystals.

CONTACT A. M. Pugachev apg@iae.nsk.su

On the other hand, local electric fields in PNR can induce anomalies of elastic modulus (C_{ij}) in a wide temperature range above the phase transition through electrostriction effect in PMN, $BaTiO_3$, and SBN-x crystals [6,11–13]. An elastic modulus has the form $C_{ij} = \sigma_{ij}/\xi_i$, where σ_{ij} is a stress and $\xi_i = \Delta l/l$ is a strain (Δl_i and l_i are linear expansion and the length of the sample along the i-axis). Anomalies of $C_{ij}(T)$ are manifested as deviations from the linear temperature behavior of the elastic modulus in a wide temperature range, when one approaches the phase transition. A detailed description of temperature dependence of $C_{ij}(T)$ in SBN-x was given in Refs. [14,15].

An attempt to determine the relation between the SHG signal with anomalies of the acoustic modules $C_{33}(T)$ in SBN-x crystals ($x = 0.33$, 0.5, 0.61, and 0.75) was taken in Ref. [14]. The main idea was to investigate a transformation of local electric fields in PNR from conventional ferroelectric to relaxor within the same class of symmetry, which occurs in barium strontium niobates of different chemical compositions: SBN-x crystals exhibit properties of both relaxors ($x > 0.61$) and conventional ferroelectrics ($x < 0.61$) [16].

In the spirit of Ref. [13], it was proposed in Ref. [14] that dipole of polar crystalline phase changes the elastic modulus value via electrostriction:

$$\Delta C_{33}(T) = C_{33}(T) - C_{\infty} = Q\chi(T)P_d^2(T) \quad (1)$$

where P_d, Q, χ, and C_∞ are the summary dipole moment in polar regions, the electrostriction coefficient, the static dielectric susceptibility, and the linear approximation of temperature dependence of elastic modulus in the high-temperature region, respectively. Provided that P_d is proportional to $I^{(2\omega)}$, Equation (1) can be written as:

$$C_{33}(T) = C_\infty(T) - \beta I^{(2\omega)}\chi(T), \quad (2)$$

where $\beta = Q\chi(T)$ is a fitting parameter. It was shown that Equation (2) failed to describe the experimental curve $C_{33}(T)$ in SBN-x crystals. In this regard, it can be assumed that Equation (2) does not describe the experimental data for at least two reasons: either the Equation (1) is not fulfilled, or the dependence of the signal of the second harmonic on polarization is more complex.

It is known that random local electric fields cause strain anomalies $\Delta\xi(T)_{ij}$, which are also proportional to P_d^2 [7,12]:

$$\Delta\xi_{ij}(T) = \xi_{ij}(T) - \xi_\infty(T) \sim Q_{ij}\ P_d^2 \quad (3)$$

where $\xi_\infty(T)$ is a linear approximation of a temperature dependence of a strain in the high-temperature region. Thus, if polar nanoregions in the paraelectric phase of the investigated crystals lead to the anomalies of the strain and elastic modules, which are proportional to P_d^2, the dependences of $\Delta\xi(T)$ and $\Delta C(T)$ would be similar. In the present paper, temperature dependences of $\xi_{33}(T)$ and $C_{33}(T)$ obtained from dilatometry and Brillouin experiments, respectively, will be compared in SBN-x crystals.

It should be noted that the dependence of SHG signal on polarization is complex: in ferroelectric phase $I^{(2\omega)} \sim P_s^2$, while in paraelectric phase $I^{(2\omega)} \sim P_d^2$ (P_s=0). In a vicinity of the phase transition (this temperature range can be large enough for ferroelectrics with a diffuse phase transition), not only short-lived local regions with dipole moment P_d, but also relatively long-lived large regions can make a contribution to the nonlinear optical signal.

In the present article, when analyzing the temperature dependence of SHG, we plan to take into account both the temperature dependences of P_s, known from other papers, and the dependences of $P_d(T)$ obtained from Brillouin scattering and dilatometry experiments.

2. Experimental

Crystals of nominally pure barium strontium niobate (SBN-x) with chemical formula $Sr_xBa_{1-x}Nb_2O_6$ ($x = 0.33$, 0.5, 0.61, and 0.75) were grown in the Institute of General Physics according to a modified Stepanov technique [17]. Samples were prepared in the form of parallelepipeds $2 \times 3 \times 5\,\text{mm}^3$ in size, cut along the crystallographic axes X, Y, and Z, respectively.

Thermal expansion was studied along the ferroelectric axis Z in crystalline samples SBN-x with in the temperature range 100-750K using NETZSCH DIL-402C induction dilatometer in a dynamic regime with heating and cooling rates of 2-3 K/min. Measurements were carried out by dry helium purging (50 ml/min). Volume concentration of oxygen was not more than 0.05%. The rod load on the sample was about 30 cN. To calibrate the thermal expansion of the measuring system, fused silica standards were used. For each of the samples, several (2–3) series of measurements were performed.

Elastic properties of the samples were investigated by Brillouin light scattering experiments. Brillouin scattering spectra were measured in back-scattering geometry $Z(XX)\bar{Z}$ in a wide temperature range including ferroelectric and paraelectric phases with the spectral resolution about 1 GHz. A solid-state single frequency laser (wavelength of 532 nm, power of 100 mW) and a six-pass Fabry-Perot interferometer were used. Elastic module components C_{33} were found as $C_{33} = \rho\, u_{33}{}^2$, where ρ is the density of the crystal and u_{33} is the sound velocity. For the back-scattering geometry, the sound velocity can be calculated by the relation $u_{ij} = \lambda \nu_{ij}/2n$ [11], where λ is the light wavelength and n is the refractive index.

SHG signal was excited by a pulsed laser with a wavelength of 1064 nm (repetition rate of 1 kHz, pulse duration of 0.6 ns, and an average power of 100 mW). The SHG signal was recorded in a back-scattering geometry by a TriVista 777 spectrometer with a spectral resolution better than $1\,\text{cm}^{-1}$. The detailed description of the SHG measurement technique was given in Ref. [18]. To study temperature dependences of elastic modules and SHG signals, a Linkam nitrogen cryostage was used.

Typical Brillouin spectra, temperature dependences of Brillouin shifts, and SHG signals in SBN-x crystals were demonstrated in Refs. [14,15]. All experiments were performed in zero-field cooling (ZFC) and zero-field heating (ZFH) regimes. Before each measurement, several cycles of ZFC and ZFH were performed.

3. Results and discussion

For visual comparison of temperature dependences of the second optical harmonic generation signals $I^{(2\omega)}_{\text{norm}}(T)$, elastic modules $C_{33}(T)$, and strain $\xi_{33}(T)$, these values are given on the same temperature scale in the Figure 1a–c. $I^{(2\omega)}_{\text{norm}}(T)$ is the second harmonic

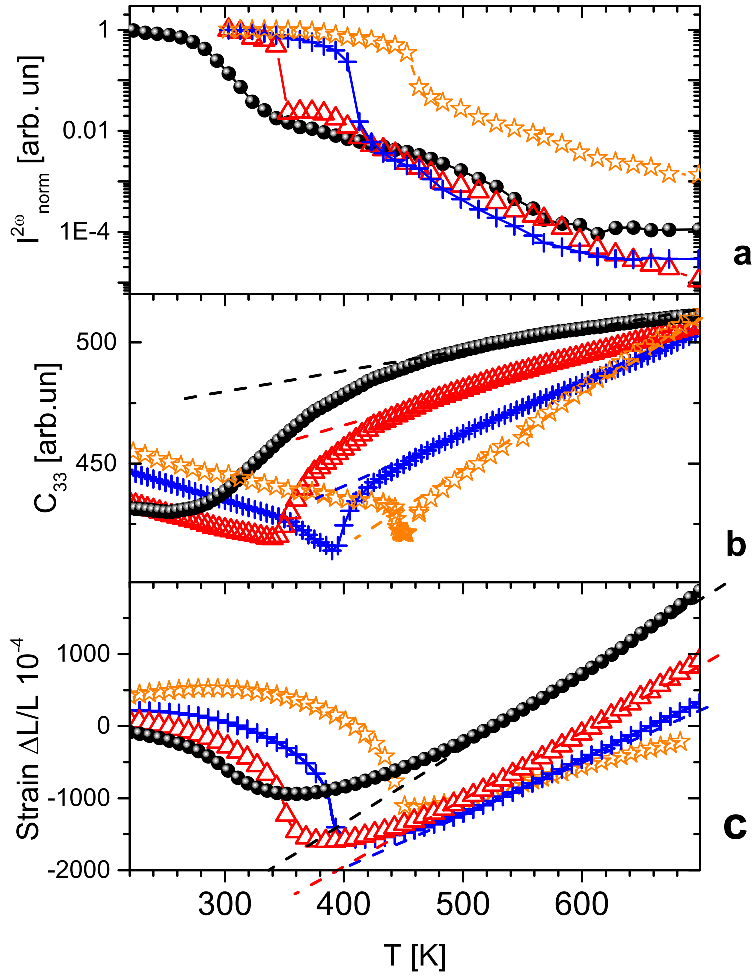

Figure 1. Temperature dependences of (a) the normalized signal of SHG $I^{2\omega}_{norm}$, (b) elastic modules C_{33} and (c) strain ξ_3 for the $Sr_xBa_{1-x}Nb_2O_6$ crystals with different chemical compositions x: (a) 0.33 (open stars), 0.5 (crosses); (b) 0.61 (open triangles), 0.75 (circles). Dash lines denote the linear approximations of temperature dependences of elastic module C_∞ and strain ξ_∞ in the high-temperature ranges.

signal normalized to the corresponding signal far below the phase transition. $I^{(2\omega)}_{\mathrm{norm}}(T)$ and C_{33} (T) dependences were presented earlier in Ref. [14], but in other scales.

The temperature dependences of $\xi_{33}(T)$ are similar to the temperature behavior of elastic modules $C_{33}(T)$: starting from some temperatures, both $\xi_{33}(T)$ and $C_{33}(T)$ deviate from linear dependences. These deviations are stronger and are manifested in a broader temperature range, when the Sr content increases. $\xi_{11}(T)$ and $C_{11}(T)$ components are not sensitive to the phase transition for all crystals studied.

We analyzed the deviations of the strain and elastic modules from the high temperature linear behavior via Equations (2) and (3) to obtain P_d. To compare the temperature dependences of $\Delta\xi_{33}(T)$, $\Delta C_{33}(T)$, and $I^{(2\omega)}(T)$, each value was normalized to temperature independent values of ξ_0, C_0, and $I_0^{(2\omega)}$ so that $\Delta\xi_{33}(T)$, $\Delta C_{33}(T)$, and $I^{(2\omega)}(T)$

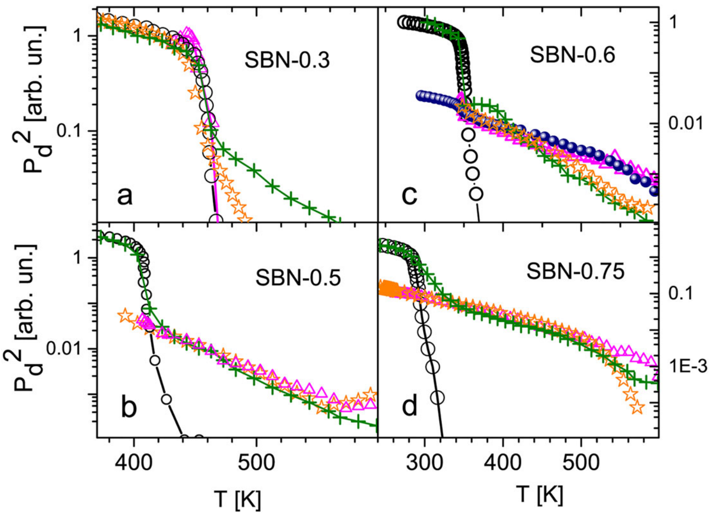

Figure 2. Temperature dependences of normalized values of spontaneous polarization taken from Ref. [19] (open circles), SHG signal (crosses), anomalies of elastic modules ΔC_{33} (open triangles), and strain $\Delta\xi_3$ (stars) for the $Sr_xBa_{1-x}Nb_2O_6$ crystals with different chemical compositions x: (a) 0.33, (b) 0.5, (c) 0.61, and (d) 0.75. Solid circles in Figure 2c denote a normalized dependence of $P_{2d}(T)$ defined in Ref. [6] from the deviation of the refractive index from linear function.

would be as close as possible at temperatures above the phase transition. The results are plotted in Figure 2.

The temperature dependences of spontaneous polarization P_s were taken from Ref. [19]. Figure 2 shows the dependence of $P_s(T)$ normalized to a temperature-independent constant P_{s0} so that the value of $P_s(T)/P_{s0}$ in the ferroelectric phase coincides with the normalized SHG signal.

Data demonstrated in Figure 2 show two pronounced temperature ranges in the dependence of $I^{(2\omega)}(T)$:

1. In the ferroelectric phase in all investigated crystals SBN-x ($x = 0.33$, 0.5, 0.61, and 0.75) the temperature dependences of SHG signal and spontaneous polarization are similar. This feature of SHG has been repeatedly noted in a number of other papers, books, and reviews [1,3].
2. At temperatures above the phase transition, spontaneous polarization disappears, whereas the second harmonic generation signal (or hyper-Rayleigh light scattering) reflects the temperature dependence of dipole moments in local asymmetric regions.

These two temperature ranges in the SHG behavior are especially distinctive for SBN-0.61/0.75 crystals, which are usually referred to ferroelectrics with a diffuse phase transition, but they are also clearly present in crystals, which are attributed to conventional ferroelectrics ($x = 0.33$, 0.5).

In addition to mentioned above two intervals in the temperature dependence of $I^{(2\omega)}(T)$ in SBN-0.5-0.75, intermediate temperature ranges are clearly demonstrated in the vicinity of the phase transition (Figure 2c,d). In these temperature ranges in the absence of macroscopic spontaneous polarization, $I^{(2\omega)}(T)$, most likely, is caused by relatively large and long-lived polar asymmetric regions [4]. In the conventional ferroelectric crystal SBN-0.3, the temperature range, in which abnormal behavior is observed, is very small and it was not possible to register this “intermediate range.”

In the pioneering works, in which the PNR was discovered [5,6], the temperature dependence $P_d(T)$ was determined from the deviation of the refractive index from linear function. The normalized dependence of $P_d(T)$ defined in Ref. [6] is presented in Figure 2. It is clearly seen that these data coincide satisfactorily with those obtained from temperature dependences of strain, elastic modules, and SHG.

4. Conclusion

In SBN-x crystals covering the conventional ferroelectric ($x = 0.5$, 0.33) and the relaxor-like ($x = 0.75$, 0.61) compositions, temperature dependences of spontaneous polarization, strain, elastic modules, and second optical harmonic generation signal are compared.

It is shown that in the temperature ranges below the ferroelectric phase transition the temperature dependences of SHG signal and spontaneous polarization are similar. At temperatures above the phase transition temperature, dependences of SHG follow appropriate dependences of anomalies of strain and elastic modules. The latter, in turn, are determined by random electric fields in local polar regions. Thus, the second harmonic generation signal in paraelectric phase describes the temperature dependences of random electric fields in polar nanoregions. In the paraelectric phase in the vicinity of the phase transition, the temperature dependences of $I^{(2\omega)}(T)$ in SBN-0.5-0.75 demonstrate an intermediate temperature range. It is proposed that SHG in these temperature ranges reflects the temperature behavior of relatively large and long-lived polar asymmetric regions.

Acknowledgments

Some part of the experiments was performed in the multiple-access center “High-Resolution Spectroscopy of Gases and Condensed Matter” in IA&E SBRAS (Novosibirsk, Russia).

Funding

This work was supported by the Russian Foundation for Basic Research, projects no. 18-02-00399 and 19-42-543-016 and State assignment No AAAA-A17-117052410033-9.

References

[1] M. E. Lines, and A. M. Glass, *Principles and Applications of Ferroelectrics and Related Materials* (Clarendon, Oxford, 1977).
[2] Y. R. Shen, *The Principles of Nonlinear Optics* (Wiley, New York, 1984).
[3] H. Vogt, Study of structural phase transitions by techniques of nonlinear optics, *Appl. Phys.* 5(2), 85 (1974). DOI: 10.1007/BF00928219.
[4] A. A. Bokov, and Z.-G. Ye, Recent progress in relaxor ferroelectrics with perovskite structure, *J. Mater. Sci.* 41(1), 31 (2006). DOI: 10.1007/s10853-005-5915-7.

[5] G. Burns, and B. A. Scott, Index of refraction in 'dirty' displacive ferroelectrics, *Solid State Commun*. 13(3), 423 (1973). DOI: 10.1016/0038-1098(73)90622-4.

[6] A. S. Bhalla *et al.*, Neurgaonkar: measurements of strain and the optical indices in the ferroelectric $Ba_{0.4}Sr_{0.6}Nb_2O_6$: Polarization effects, *Phys. Rev. B* 36(4), 2030 (1987). DOI: 10.1103/PhysRevB.36.2030.

[7] D. Viehland *et al.*, Deviation from Curie-Weiss behavior in relaxor ferroelectrics, *Phys. Rev. B* 46(13), 8003 (1992). DOI: 10.1103/PhysRevB.46.8003.

[8] S. G. Lushnikov *et al.*, Anomalous dispersion of the elastic constants at the phase transformation of the $PbMg_{1/3}Nb_{2/3}O_3$ relaxor ferroelectric, *Phys. Rev. B* 77(10), 104122 (2008). DOI: 10.1103/PhysRevB.77.104122.

[9] J.-H. Ko *et al.*, Effects of Sr content and bias field on acoustic properties of strontium barium niobate studied by Brillouin light scattering, *Appl. Phys. Lett*. 99(21), 212902 (2011). DOI: 10.1063/1.3663622.

[10] G. Xu *et al.*, A neutron elastic diffuse scattering study of PMN, *Phys. Rev. B* 69(6), 064112 (2004). DOI: 10.1103/PhysRevB.69.064112.

[11] J.-H. Ko *et al.*, Precursor dynamics in the ferroelectric phase transition of barium titanate single crystals studied by Brillouin light scattering, *Phys. Rev. B* 84(9), 094123 (2011). DOI: 10.1103/PhysRevB.84.094123.

[12] L. E. Cross, Relaxor ferroelectrics, *Ferroelectrics* 76(1), 241 (1987). DOI: 10.1080/00150198708016945.

[13] W. Rehwald, The study of structural phase transitions by means of ultrasonic experiments, *Adv. Phys*. 22(6), 721 (1973). DOI: 10.1080/00018737300101379.

[14] M. Pugachev *et al.*, Comparison of acoustic and nonlinear optic properties of strontium barium niobate crystals of different compositions, *Ferroelectrics* 538(1), 126 (2019). DOI: 10.1080/00150193.2019.1569995.

[15] M. Pugachev *et al.*, Dependence of acoustic anomalies on chemical composition in strontium barium niobate crystals (from conventional ferroelectric to relaxor) probed by Brillouin light scattering, *Ferroelectrics* 542(1), 21 (2019). DOI: 10.1080/00150193.2019.1574657.

[16] T. Lukasiewicz *et al.*, Strontium-barium niobate single crystals, growth and ferroelectric properties, *J. Cryst. Growth*. 310(7-9), 1464 (2008). DOI: 10.1016/j.jcrysgro.2007.11.233.

[17] L. I. Ivleva *et al.*, Growth of SBN single crystals by Stepanov technique for photorefractive applications, *Opt. Mater*. 4(2-3), 168 (1995).

[18] A. M. Pugachev *et al.*, Broken local symmetry in paraelectric $BaTiO_3$ proved by second harmonic generation, *Phys. Rev. Lett*. 108(24), 247601 (2012). DOI: 10.1103/PhysRevLett.108.247601.

[19] A. M. Glass, Investigation of the electrical properties of $Sr_{1-x}Ba_xNb_20_6$ with special reference to pyroelectric detection, *J. Appl. Phys*. 40(12), 4699 (1969). DOI: 10.1063/1.1657277.